

# Testing Cold, Fuzzy, and Self-Interacting Dark Matter Models Using Late-Type Galactic Rotation Curves

## Introduction

Flat rotation curves at the outer galactic radii are among the observational evidence of dark matter (DM) on the galactic scale. The standard **cold dark matter (CDM)** model successfully explained the formation of the large-scale structures in the universe. However, many issues arise on the galactic scale (small-scale problems), such as the **core-cusp problem**, i.e., the discrepancy between the observed **cored** DM profile of dwarf galaxies and the predicted **cuspy Navarro-Frenk-White (NFW)** profile based on CDM simulations. This problem had motivated astronomers to propose empirical DM density profile that better matches various observations, e.g., the **Burkert** profile.

**NFW**

$$\rho_{\text{NFW}}(r) = \frac{\rho_s}{\frac{r}{r_s} \left(1 + \frac{r}{r_s}\right)^2}$$

$\rho_s$ : characteristic density  
 $r_s$ : characteristic radius

**Burkert**

$$\rho_{\text{Burkert}}(r) = \frac{\rho_s}{\left(1 + \frac{r}{r_s}\right) \left[1 + \left(\frac{r}{r_s}\right)^2\right]}$$

Another issue is the **rotation curves diversity problem**, i.e., the scatter in the inner shape of rotation curves of galaxies of similar masses is much broader than predicted by CDM simulations.

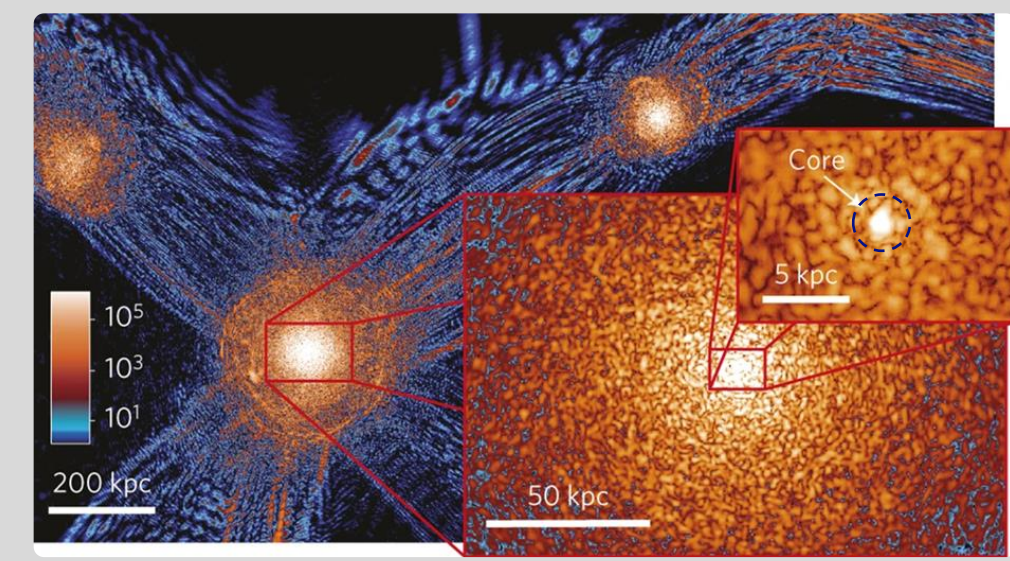
One commonly proposed solution is to use alternative DM models, e.g., **fuzzy dark matter** and **self-interacting dark matter**.

### Fuzzy Dark Matter (FDM)

- Consists of ultralight DM particles ( $10^{-24} \lesssim \frac{m_{\text{FDM}}}{\text{eV}} \lesssim 10^{-19}$ ), e.g., axion and axion-like particles (ALPs).

$$\lambda_{\text{dB}} = \frac{h}{m_{\text{FDM}} v}$$

FDM exhibit wave-like behavior on galactic scales, described by a Schrödinger-Poisson equation. Its de Broglie wavelength is in the order of  $\sim 1$  kpc.



- On the scale  $\lambda < \lambda_{\text{dB}}$ , quantum pressure provides stability against gravitational collapse, forming a constant density **soliton core** ( $\sim 0.3 - 1.6$  kpc) at the halo center, which alleviates the **core-cusp problem**.
- On the outside, quantum pressure become less significant, and FDM shows interference patterns in the form of granules and fringes which shows the DM distribution.

$$\rho_{\text{sol},0} = \frac{0.019 M_{\odot}}{m_{22}^2 \left(\frac{r_{\text{sol}}}{\text{kpc}}\right)^4 \text{pc}^3}$$

$$r_a = \alpha r_{\text{sol}} \quad m_{22} = \frac{m_{\text{FDM}}}{10^{-22} \text{ eV}}$$

$$\rho_{\text{sol},0}: \text{soliton core density}$$

$$r_{\text{sol}}: \text{soliton characteristic radius}$$

$$r_a: \text{halo transition radius}$$

Schive et al. (2014)

- The mass of FDM particle is currently have not been well constrained. The constraints from previous works are in tension with each other and are strongly inconsistent with many cosmological constraint. Further observations and simulations have to be done to get a more stringent constraint.

### Self-Interacting Dark Matter (SIDM)

- SIDM suggests interactions among DM particles with a large scattering cross section ( $\sigma/m_{\chi}$ ) due to short-range interactions or weak interactions mediated by light particles exchange.
- DM self-interactions allow **thermalization** to occur in the innermost halo region, leading to the formation of a constant density **isothermal core** ( $\sim 0.5 - 1$  kpc), solving the **core-cusp problem**. The transition radius is defined as radius  $r_1$  at which the DM particles have only interacted once in the halo's lifetime.
- Thermalization ties the core sizes and shapes of DM halos to the stars' spatial distribution, which explained the **rotation curves diversity problem**.

**SIDM**

$$\rho_{\text{SIDM}}(r) = \begin{cases} \rho_{\text{iso}}(r), & r \leq r_1 \\ \rho_{\text{NFW}}(r), & r \geq r_1 \end{cases}$$

$$\rho_{\text{iso}}(r) = \rho_0 \exp\left[\frac{\Phi_{\text{tot}}(0) - \Phi_{\text{tot}}(r)}{\sigma_v^2}\right]$$

$\rho_{\text{iso}}(r)$  is obtained by solving the Poisson's equation:

$$\nabla^2 \Phi_{\text{tot}}(r) = 4\pi G [\rho_{\text{iso}}(r) + \rho_{\text{bar}}(r)]$$

The profile transition occurs at a radius where:

$$\text{Number of interactions} \approx \frac{(\sigma v_{\text{rel}})}{m_{\chi}} \rho_{\text{iso}}(r_1) t_{\text{age}} \approx 1$$

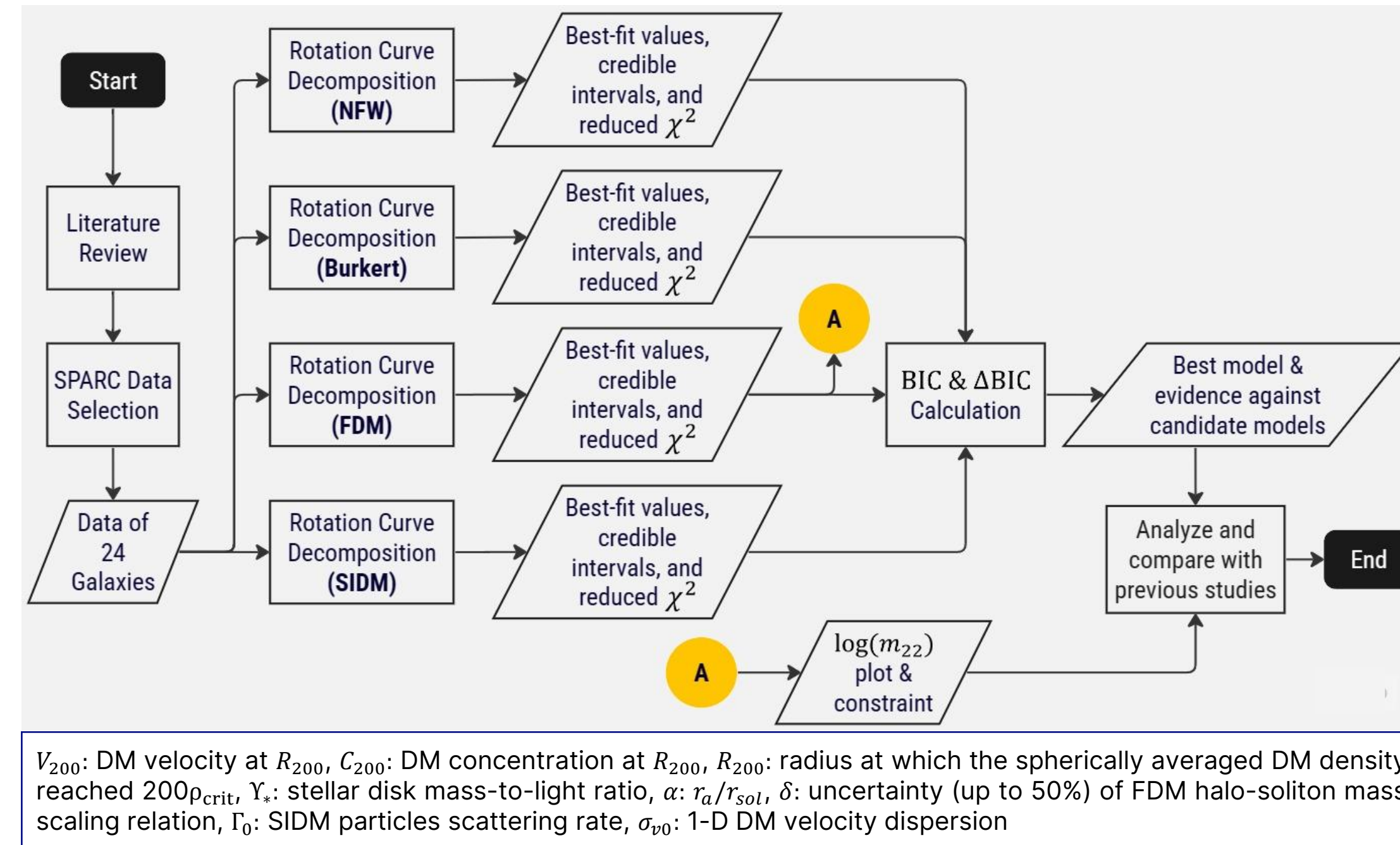
For spherical halos:

$$\langle \sigma v_{\text{rel}} \rangle = \sigma \left(\frac{4}{\sqrt{\pi}}\right) \sigma_v$$

- $t_{\text{age}}$ : age of the halo
- $v_{\text{rel}}$ : relative scattering velocity
- $\sigma_v$ : 1D velocity dispersion
- $\Phi_{\text{tot}}$ : total potential gravity
- $\rho_{\text{bar}}$ : baryon density profile
- $\rho_0$ : isothermal core central density

Ren et al. (2019) & Zentner et al. (2022)

## Methods



$V_{200}$ : DM velocity at  $R_{200}$ ,  $C_{200}$ : DM concentration at  $R_{200}$ ,  $R_{200}$ : radius at which the spherically averaged DM density reached  $200\rho_{\text{crit}}$ ,  $Y$ : stellar disk mass-to-light ratio,  $\alpha$ :  $r_s/r_{\text{sol}}$ ,  $\delta$ : uncertainty (up to 50%) of FDM halo-soliton mass scaling relation,  $\Gamma_0$ : SIDM particles scattering rate,  $\sigma_v$ : 1-D DM velocity dispersion

### SPARC Data Selection:

$$Q = 1 \quad \text{Data points} > 5 \quad M_* \leq 10^{10} M_{\odot} \quad V_{\text{flat}} \neq 0 \quad R_{\text{min}} < 0.5 \text{ kpc}$$

24 sample galaxies

- The rotation curves are decomposed into **disk**, **gas**, and **DM halo** using the Markov Chain Monte Carlo (MCMC) method in Python (the emcee package). We assumed that the DM halos have spherical symmetry.
- We followed Khelashvili et al. (2023), Ren et al. (2019) and Zentner et al. (2022) for deriving the velocity profile of the FDM and SIDM halo models.
- The free parameters used for each model are shown in the table below. We used a constant  $\sigma/m_{\chi}$  for the SIDM model ( $3 \text{ cm}^2/\text{g}$ ).
- For model comparison, we calculated BIC &  $\Delta\text{BIC}$  value from each fitting.

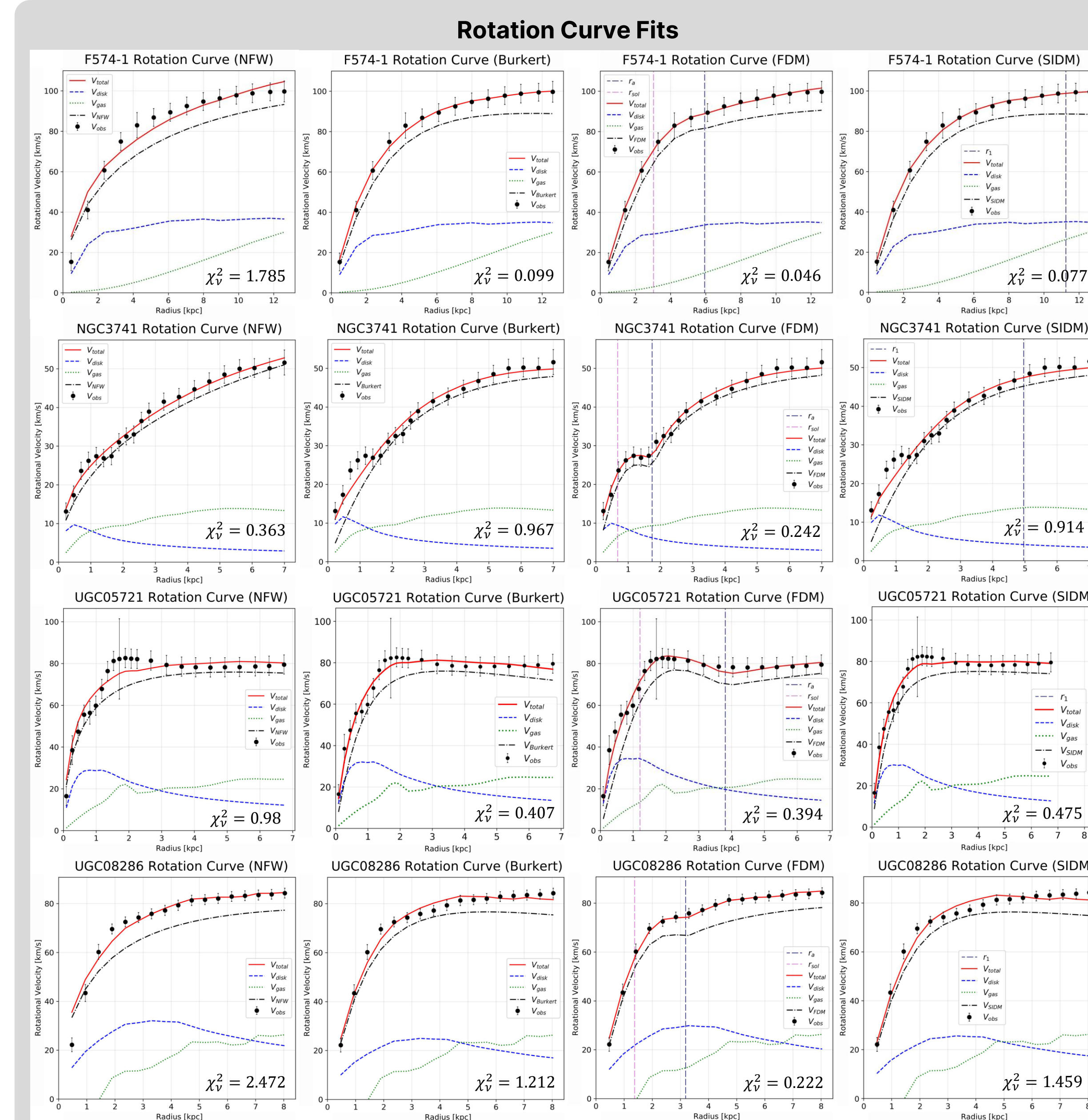
Model	Parameters
NFW	$V_{200}, C_{200}, Y,$
Burkert	$V_{200}, C_{200}, Y,$
FDM	$V_{200}, m_{22}, \alpha, \delta, Y,$
SIDM	$\Gamma_0, \sigma_v, Y,$

$$\text{BIC} = -2 \ln \mathcal{L} + k \ln N$$

$$\Delta\text{BIC} = \text{BIC}_{\text{alternative}} - \text{BIC}_{\text{best}}$$

$\mathcal{L}$ : maximum likelihood,  $k$ : number of free parameters,  $N$ : number of data points

## Results

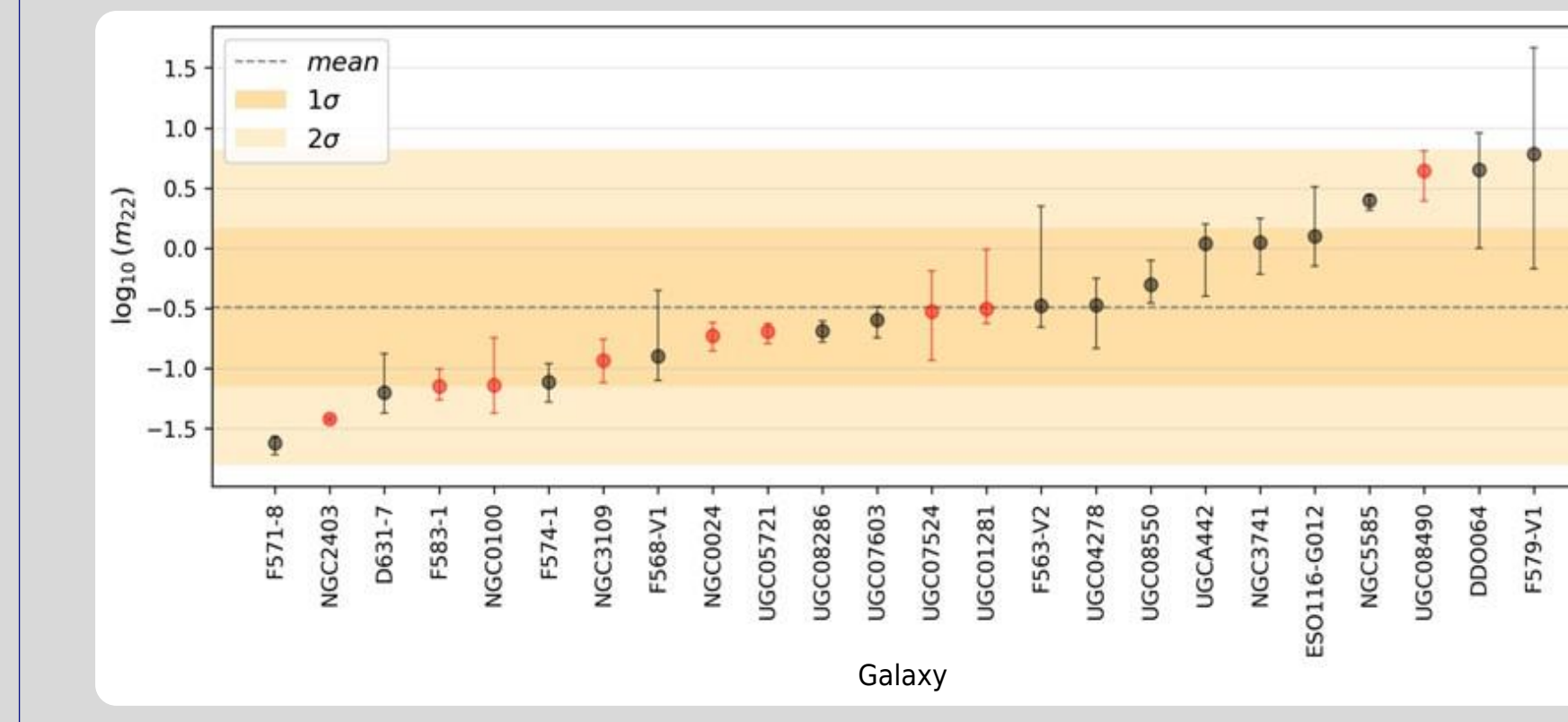


Rotation curve fits of 4 of the sample galaxies using NFW, Burkert, FDM, and SIDM halo models.

- Generally, **NFW** halo (average  $\chi^2$  of 2.146) produces total rotation curves model that are too high in the inner radii due to the cuspy nature of the halo.
- Burkert** halo (average  $\chi^2$  of 1.092) produces fits that matches the data better in the inner radii than NFW. However, for some galaxies it fits quite worse at the outer radii.
- FDM** halo (average  $\chi^2$  of 0.529) produces the best fits for most of the galaxies. Some galaxies that have a "sharp" turn on their rotation curves can be fitted well using the FDM halo by the presence of soliton-NFW transition. The soliton's characteristic radius ( $r_{\text{sol}}$ ) and transition radius ( $r_a$ ) have an average of 1.89 kpc and 3.62 kpc, respectively.
- Visually, **SIDM** halo (average  $\chi^2$  of 1.16) produces similar fits as the Burkert halo in most cases. For many galaxies, it produces an isothermal core-NFW transition far at the outer radii, even outside of the SPARC's data points, which agrees with the results of a previous work (Loizeau et al., 2021). In these cases, it indicates that the observational data can be sufficiently fitted using a pure isothermal halo model. The transition radius ( $r_1$ ) have an average of 10.64 kpc.

- Based on the **BIC** values, 10 galaxies support the Burkert model, 9 galaxies support the SIDM model, and 5 galaxies support the NFW model.
- Despite the remarkable fits, none of the galaxies in the sample supports the FDM model.
- Based on the **ΔBIC** values, there are **positive** evidence and **strong** evidence to **reject** the FDM model from **15** and **9** galaxies, respectively.
- There is only one positive evidence to reject each of the NFW, Burkert, and SIDM model, and one strong evidence to reject the NFW model.

### FDM Particle Mass

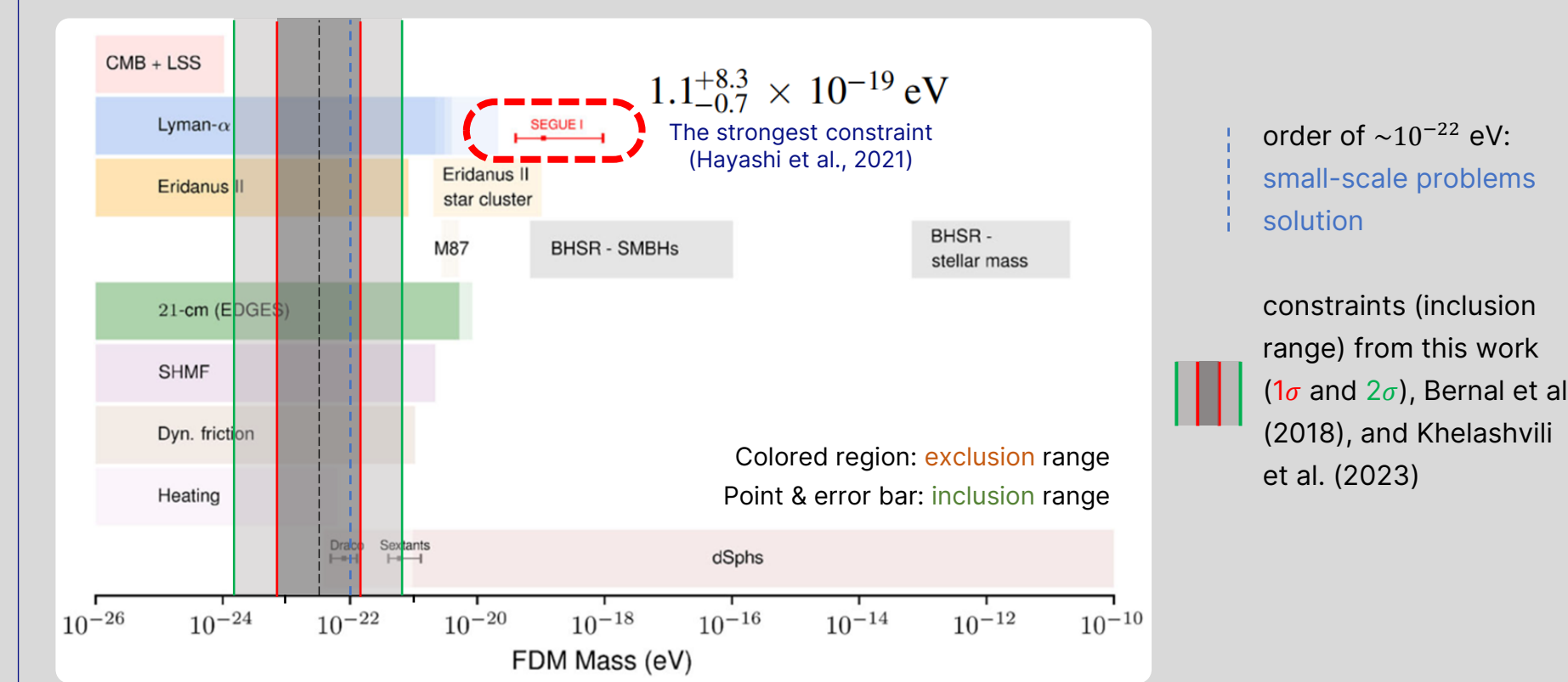


MAP (Maximum A Posteriori) values and 95% credible intervals of  $\log m_{22}$  from the 24 sample galaxies.

$$m_{\text{FDM}}(1\sigma) = 0.322^{+1.141}_{-0.251} \times 10^{-22} \text{ eV}$$

$$m_{\text{FDM}}(2\sigma) = 0.322^{+6.324}_{-0.307} \times 10^{-22} \text{ eV}$$

- Based on the rotation curves fitting, we obtained a constraint on the FDM particle mass as above. The 95% credible intervals of the mass are in tension for different individual galaxies, which agrees with the results of a previous work (Khelashvili et al., 2023).



FDM particle mass constraints from various astrophysical observations (Ferreira, 2021), this work, Khelashvili et al. (2023), and Bernal et al. (2018).

- The constraint set from this work is strongly inconsistent with various astrophysical observations. It is also inconsistent with the strongest constraint to date ( $1.1^{+8.3}_{-0.7} \times 10^{-19} \text{ eV}$ ), which is obtained from dynamical analysis of an ultrafaint dwarf, Segue I (Hayashi et al., 2021).

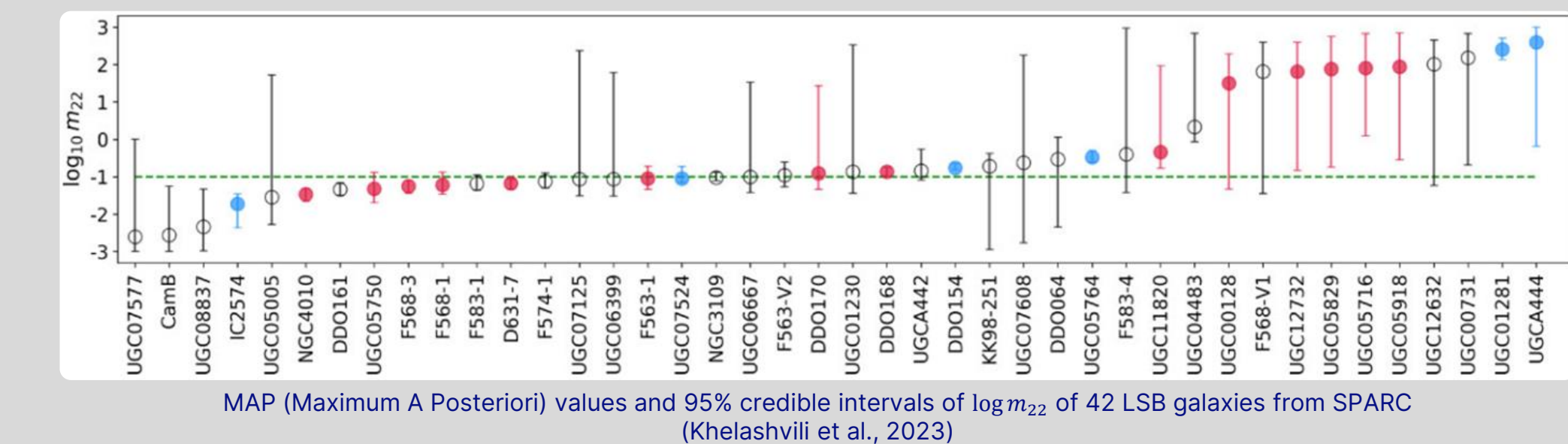
## Discussion & Conclusions

### Rotation Curve Fits

- For many galaxies, the reduced chi-squared ( $\chi^2_{\nu}$ ) values obtained from the rotation curves fitting were not representing the fit qualities well, due to the wide uncertainties on the data points. Therefore, the BIC value was chosen for model comparison.
- The fits using the FDM halo model are strongly penalized by the BIC, probably due to the high complexity of the model. In this work, we used 5 free parameters ( $k = 5$ ) for the FDM model, contrast to the three other models with only 3 free parameters ( $k = 3$ ). As from the formula, BIC penalize models with a higher number of free parameters ( $k$ ). Using a more simplified model of FDM might be useful for a "fairer" comparison, if the constraints on the model had been more stringent.

### FDM Particle Mass

- The constraints on FDM particle mass of this work overlap with the results from Khelashvili et al. (2023) ( $m_{\text{FDM}} \approx 10^{-23} \text{ eV}$ ). There are some differences on the 95% credible intervals for some overlapping galaxies, due to the additional free parameters used in the latter work (distance and inclination of the galaxies).



- Bernal et al. (2018) fitted the rotation curves of 18 LSB galaxies and 6 NGC galaxies (4 of them are from the SPARC catalog). They also found that the constraints from each galaxy did not overlap. Based on individual galaxies analysis, they obtained a constraint in the range:  $2.12 \times 10^{-24} < m_{\text{FDM}}/\text{eV} < 2.7 \times 10^{-22}$
- Based on combined analysis (all of the galaxies are fitted simultaneously), they obtained a best-fit value:  $m_{\text{FDM}} = 5.54 \times 10^{-24} \text{ eV}$

### Conclusions:

- For the standard **CDM** model, the Burkert model fits most galaxies better than NFW. Based on the BIC value, Burkert is the most supported model (10 galaxies), while NFW was only supported by 5 galaxies.
- The **FDM** model produces the best fits for most of the galaxies. However, it is rejected by all galaxies based on the  $\Delta\text{BIC}$  criterion, due to penalties on the BIC value because of the high complexity of the model (5 free parameters).
- For most galaxies, the **SIDM** model produces similar fits to those of the Burkert model. Based on the BIC value, it received the most support after Burkert (9 galaxies). It can explain the rotation curves diversity problem in the samples.
- Based on the fitting results, we obtained a constraint on the FDM particle mass which overlaps with the results of Bernal et al. (2018) and Khelashvili et al. (2023). However, it contradicts various astrophysical observations.

## References

Bernal, T., Fernández-Hernández, L. M., Matos, T., & Rodríguez-Meza, M. A. (2018). Rotation curves of high-resolution LSB and SPARC galaxies with fuzzy and multistate (ultralight boson) scalar field dark matter. *Monthly Notices of the Royal Astronomical Society*, 475, 1447–1468.

Ferreira, E. G. M. (2021). Ultra-light Dark Matter. *The Astronomy and Astrophysics Review*, 29, 186.

Hayashi, K., Ferreira, E. G. M., & Chan, H. Y. J. (2021). Narrowing the Mass Range of Fuzzy Dark Matter with Ultrafaint Dwarfs. *The Astrophysical Journal Letters*, 912, 5.

Jiang, F., Benson, A., Hopkins, P. F., Slone, O., Lisanti, M., Kaplinghat, M. et al. (2023). A semi-analytic study of self-interacting dark-matter halos with baryons. *Monthly Notices of the Royal Astronomical Society*, 521, 4630–4644.

Khelashvili, M., Rudakovskiy, A., & Hossenfelder, S. (2023). Dark matter profiles of SPARC galaxies: a challenge to fuzzy dark matter. *Monthly Notices of the Royal Astronomical Society*, 523, 3393–3405.

Lelli, F., McGaugh, S. S., & Schombert, J. M. (2016). SPARC: Mass Models for 175 Disk Galaxies with Spitzer Photometry and Accurate Rotation Curves. *The Astronomical Journal*, 152, 1–14.

Loizeau, N., & Farrar, G. R. (2021). Galaxy Rotation Curves Disfavor Traditional and Self-interacting Dark Matter Halos, Preferring a Disk Component or Einasto Function. *The Astrophysical Journal Letters*, 920, 20.

Ren, T., Kwa, A., Kaplinghat, M., & Yu, H.-B. (2019). Reconciling the Diversity and Uniformity of Galactic Rotation Curves with Self-Interacting Dark Matter. *Physical Review X*, 9, 12.

Schive, H.-Y., Chiueh, T., & Broadhurst, T. (2014). Cosmic Structure as the Quantum Interference of A Coherent Dark Wave. *Nature Physics*, 10, 496–499.

Spergel, D. N. & Steinhardt, P. J. (2000). Observational Evidence for Self-Interacting Cold Dark Matter. *Physical Review Letters*, 84(17), 3760–3763.

Zentner, A., Dandavate, S., Slone, O., & Lisanti, M. (2022). A critical assessment of solutions to the galaxy diversity problem. *Journal of Cosmology and Astroparticle Physics*, 2022, 25.



Scan for more details about our research.